

Supporting Information for

Peroxidase-like activity of Acetylcholine based colorimetric detection of Acetylcholinesterase activity and inhibitor Organophosphorus

Ting Han, Guangfeng Wang*

Key Laboratory of Chem-Biosensing, Anhui province; Key Laboratory of Functional Molecular Solids, Anhui province; College of Chemistry and Materials Science, Center for Nano Science and Technology, Anhui Normal University, Wuhu 241000, PR China

*Corresponding Author: Guangfeng Wang

E-mail: wangyuz@mail.ahnu.edu.cn

Fax: +86-553-3869303; Tel: +86-553-3869302

Contents

- 1. Optimization of experimental conditions**
- 2. Reaction kinetics**
- 3. Supporting figures and tables**

1. Optimization of experimental conditions

To choose the optimal conditions for Ops detection based on the AChE-TMB-H₂O₂ system, some key factors including pH, reaction temperature, and reaction time should also be carefully considered. This colorimetric process was pH-dependent due to peroxidase-like activity of ATCh, and so the effect of various pH values was evaluated first. The results show that the absorbance intensity of the response increased first with the increase of the pH value and further decreased if the pH was higher than 7.4 (Fig. S1A). When the pH level was higher than 8, the response became weaker than that at pH 7, which may be ascribed to the fact that the formation is hydrolysis of ATCh. The obvious response is obtained at pH 7.4, and this is therefore adopted in the following experiments. The effect of the reaction time between ATCh and TMB-H₂O₂ was also studied. As shown in Fig. S1B, one can find that the absorbance intensity at 652 nm increase sharply with the increase of reaction time, which tended to be constant after 5 min. To make all ATCh inactivated by Ops, a slightly longer time was needed to complete the reaction, thus a 7 min reaction time was used.

Temperature is another crucial factor for most enzyme-based systems. Fig. S1C displays that the absorbance increases with increasing temperature in the range 5 °C to 40 °C. Further increases in temperature result in the decrease of absorbance. Accordingly, 37 °C is adopted as the optimal reaction temperature.

2. Reaction kinetics

In order to illustrate the performance of ATCh, kinetic measurements were carried out by monitoring the absorbance change at 652 nm. The Michaelis Menten constant (K_m) and catalytic constant (K_{cat}) were calculated using Lineweaver Burk plots of the double reciprocal of the Michaelis-Menten equation. (Michaelis et al. 2011)

In the kinetic assays, TMB and H_2O_2 were firstly added into 10 mM PBS buffer (pH 7.4) at a certain concentration. Then ATCh complex was added into the working solution to initiate the reaction. All the experiments were repeated at least thrice for reproducibility. The initial velocities (v) were calculated according to Eqs. (1) and (2)

$$C_p = A_{652} / \epsilon L \quad (1)$$

$$v = \frac{dC_p}{dt} \quad (2)$$

Where C_p represents the concentration of oxTMB, ϵ is the extinction coefficient of oxTMB, L is the optical path length of 1cm. In order to calculate the enzymatic parameters, serial concentrations of TMB or H_2O_2 was done using PBS buffer at pH 7.4. The kinetic parameters were determined via Michaelis–Menten Eq. (3)

$$v = \frac{V_{max}[S]}{K_m + [S]} \quad (3)$$

where v is the initial velocity of the reaction, V_{max} is the maximal rate of reaction, $[S]$ is the substrate concentration, and K_m is the Michaelis–Menten constant.

K_m and V_{max} were obtained by Lineweaver–Burk plot method according to Eq. (4):

$$\frac{1}{v} = \frac{K_m}{V_{max}} + \frac{1}{V_{max}[S]} \quad (4)$$

The result was shown in Fig.S2 and Table S1, which indicated that ATCh possessed excellent catalytic efficiency.

3. Supporting figures and tables

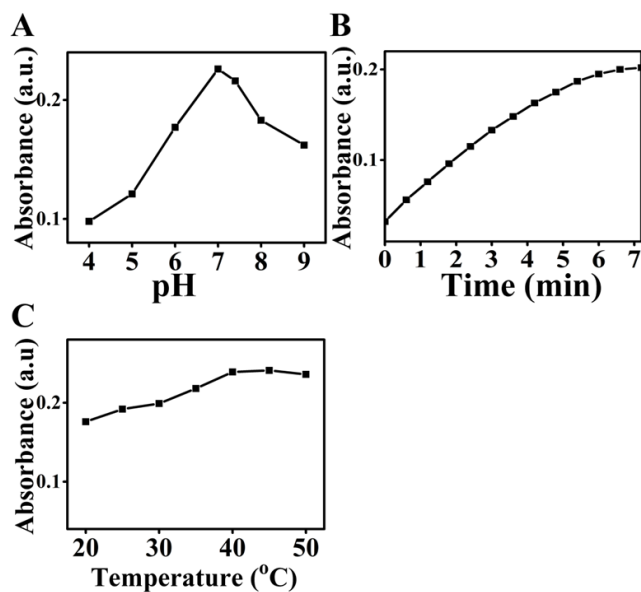


Figure S1 Real-time absorbance changes at 652 nm recorded of ATCh-TMB-H₂O₂ system with different pH (4, 5, 6, 6, 7, 7.4, 8, 8, 9) (A), reaction time (60, 120, 180, 240, 300, 360 and 720 s) (B), and temperature (from 20 to 50 °C) (C).

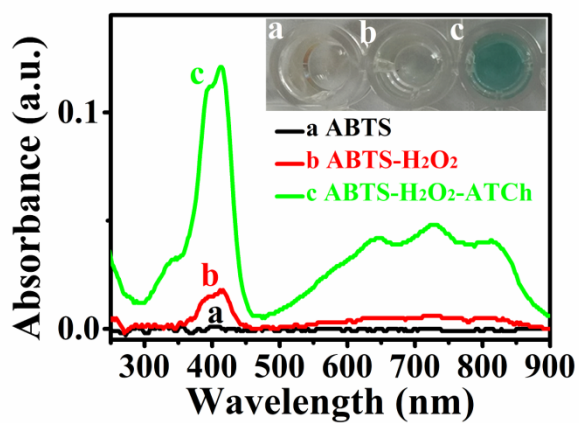


Figure S2 UV-vis spectra of the sensing system under different conditions, 0.5 mM ABTS (a) with 0.25mM H₂O₂ (b, c) and 0.5 mM ATCh (c)

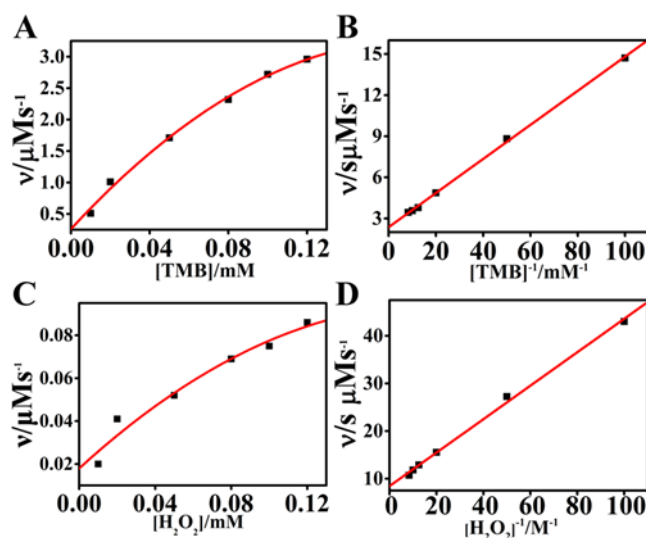


Figure S3 (A) Steady-state kinetic assay and catalytic mechanism of ATCh, and the initial velocities in the oxidization of TMB in the presence of H₂O₂ measured at pH 7.4 and 25 °C with the fixed concentration of H₂O₂ and varied concentration of TMB and the concentration of TMB fixed at 0.25 mM and the H₂O₂ concentration varied (C). (B) and (D) are the double-reciprocal plots of (A) and (C), respectively.

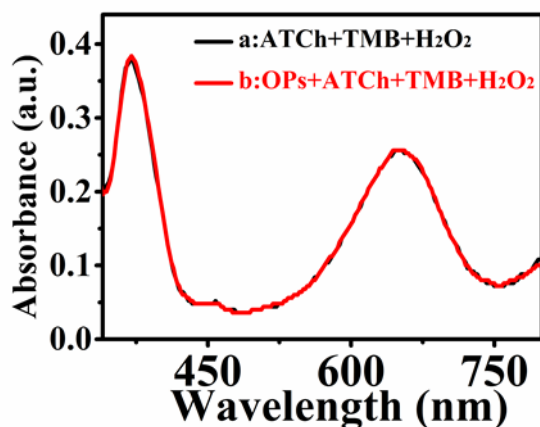


Figure S4 The influence of paraoxon on ATCh-TMB-H₂O₂ system. The concentration of paraoxon, ATCh and TMB were 120.0 μg/mL, 0.5 mM and 0.1 mM, respectively.

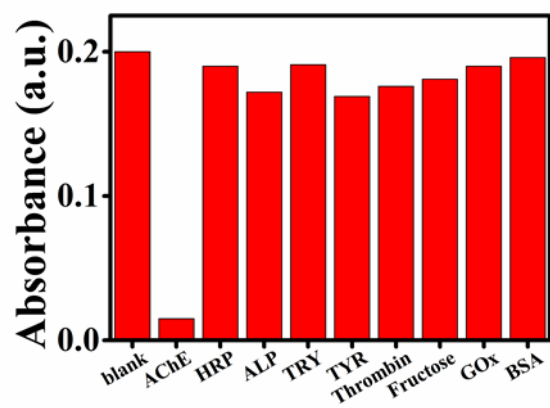


Figure S5 Investigation of the selective recognition capability of the proposed colorimetric assay for AChE over other nonspecific proteins and enzymes.

Table 1. Comparison with other enzyme mimetics

Enzyme	Substrate	$K_m(\text{mM})$	$U_{\max} \times 10^{-8}$ (Ms^{-1})	Reference
MoS ₂	TMB	0.525	5.16	1
nanosheets	H ₂ O ₂	0.0116	4.29	
Fe ₃ O ₄	TMB	0.098	3.44	2
	H ₂ O ₂	154	9.78	
C-Dots	TMB	0.039	3.61	3
	H ₂ O ₂	26.77	30.61	
Pd NPs/GNs	TMB	0.39	35.02	4
	H ₂ O ₂	23.9	13.66	
Cu nanocluster	TMB	0.648	5.96	5
	H ₂ O ₂	29.16	4.22	
BSA-Pt	TMB	0.119	21	6
	H ₂ O ₂	41.8	16.7	
CoO ₄	TMB	0.037	6.27	7
	H ₂ O ₂	140.07	12.1	
GQD	ABTS	10.04	1.78	8
	H ₂ O ₂	1.17	1.24	
FePt-Au HNPs	TMB	0.445	24.67	9
	H ₂ O ₂	0.0185	0.6894	
GO-COOH	TMB	0.0237	3.45	10
	H ₂ O ₂	3.99	3.85	
Au/Co ₃ O ₄ -CeO _x	TMB	0.1219	0.8577	11
	H ₂ O ₂	0.2724	0.3898	
FePt/GO	TMB	2.953	162.87	12
	H ₂ O ₂	0.0128	1.1598	
H ₂ TCPP-NiO	TMB	1.14×10^{-5}	48.2	13
	H ₂ O ₂	0.0391	1.38	
TiO ₂ NTA	TMB	0.127	7.02	14
	H ₂ O ₂	5.26	760	
G20-Cu(II)	TMB	0.257	24.29	15
	H ₂ O ₂	102.3	25.67	
BSA-Au	TMB	0.00253	6.23	16
	H ₂ O ₂	25.3	7.21	
ATCh	TMB	0.104	13.86	This work
	H ₂ O ₂	87.2	15.33	

Table 2. Comparison of the proposed method with other methods for AChE detection

Method	Linear range (mU/mL)	Detection Limit (mU/mL)	Reference
Metal coordination polymer		0.04	17
C ₃ N ₄ nanodots	0.01-3	0.01	18
Resurfaced Fluorescent Protein	0.025-2	0.015	19
Gold nanoclusters	5-150	0.02	20
Quantum dots	10-1000	10	21
DNA-templated copper/silver nanoclusters	0.05-2.0	0.05	22
MnO ₂ nanosheets	0.1-15	0.035	23
Colorimetric assay	2.0-14	0.5	This work

Table 3. Comparison of the proposed method with other methods for Ops detection

Method	Linear range (ng/mL)	LOD (ng/mL)	References
Electrochemical immunosensor	2-2500	2	24
Carbon dots-based sensor	0.026-26300	0.013	25
QDs-based sensor	25-3000	18.0	26
Enzyme-linked immunosorbent assay	44-1380	18.9	27
Fe ₃ O ₄ imprinted polymers	15-2500	5.2	28
Electrochemical sensor	5-3000	2.0	29
AuNPs-based methods	0.13-132	0.026	30
Optical microbial sensor	1053-21057	78.9	31
Gas chromatography	30-1000	10	32
Nanoceria-coated paper	0-120	14	33
DNA conformational switch	10-10000	2.1	34
Biosensor using MPH enzyme	0-26312	1052.8	35
ATCh minic enzyme	10-140	4.0	This work

Table 4. Analytical application

Carrot and peach samples were purchased from the local market and practical applications of this approach for real sample assay were investigated by monitoring the traces of Ops.

The designed system exhibited good recovery ranging from 97.52% to 116.2% for (Organophosphate) spiked real samples, which is in the recovery range permitted by Chinese National Standards (GB/T 27404-2008). Thus, the proposed homogeneous colorimetric analytical strategy exhibits great promise for practical applications.

<i>Food samples</i>	<i>No.</i>	<i>Ops added (μg/L)</i>	<i>Ops detected (μg/L)</i>	<i>Recovery (%)</i>	<i>Standards for recovery (%)</i>
<i>Peach</i>	<i>1</i>	<i>10</i>	<i>11.12</i>	<i>111.20%</i>	<i>60-120</i>
	<i>2</i>	<i>100</i>	<i>109.8</i>	<i>109.80%</i>	<i>60-120</i>
	<i>3</i>	<i>200</i>	<i>210.5</i>	<i>105.25%</i>	<i>60-120</i>
	<i>4</i>	<i>500</i>	<i>487.6</i>	<i>97.52%</i>	<i>80-110</i>
	<i>5</i>	<i>1000</i>	<i>1008.9</i>	<i>100.89%</i>	<i>80-110</i>
<i>Carrot</i>	<i>1</i>	<i>10</i>	<i>11.62</i>	<i>116.20%</i>	<i>60-120</i>
	<i>2</i>	<i>100</i>	<i>106.7</i>	<i>106.70%</i>	<i>60-120</i>
	<i>3</i>	<i>200</i>	<i>212.5</i>	<i>106.25%</i>	<i>60-120</i>
	<i>4</i>	<i>500</i>	<i>491.7</i>	<i>98.34%</i>	<i>80-110</i>
	<i>5</i>	<i>1000</i>	<i>1009.8</i>	<i>100.98%</i>	<i>80-110</i>

$$\text{Recovery (\%)} = (C_{\text{detected}} / C_{\text{added}}) \times 100\%$$

Chinese National Standards (GB/T 27404-2008)

References

1. T. Lin, L. Zhong, L. Guo, F. Fu and G. Chen, *Nanoscale*, 2014, **6**, 11856-11862.
2. L. Gao, J. Zhuang, L. Nie, J. Zhang, Y. Zhang, N. Gu, T. Wang, J. Feng, D. Yang, S. Perrett and X. Yan, *Nat. Nanotechnol.*, 2007, **2**, 577-583.
3. W. Shi, Q. Wang, Y. Long, Z. Cheng, S. Chen, H. Zheng and Y. Huang, *Chem. Commun.*, 2011, **47**, 6695-6697.
4. X. Chen, B. Su, Z. Cai, X. Chen and M. Oyama, *Sens. Actuators. B Chem.*, 2014, **201**, 286-292.
5. L. Hu, Y. Yuan, L. Zhang, J. Zhao, S. Majeed and G. Xu, *Anal. Chim. Acta*, 2013, **762**, 83-86.
6. W. Li, B. Chen, H. Zhang, Y. Sun, J. Wang, J. Zhang and Y. Fu, *Biosens. Bioelectron.*, 2015, **66**, 251-258.
7. J. Mu, Y. Wang, M. Zhao and L. Zhang, *Chem. Commun.*, 2012, **48**, 2540-2542.
8. H. Sun, A. Zhao, N. Gao, K. Li, J. Ren and X. Qu, *Angew. Chem. Int. Ed.*, 2015, **54**, 7176-7180.
9. Y. Ding, B. Yang, H. Liu, Z. Liu, X. Zhang, X. Zheng and Q. Liu, *Sens. Actuators. B Chem.*, 2018, **259**, 775-783.
10. Y. Song, K. Qu, C. Zhao, J. Ren and X. Qu, *Adv. Mater.*, 2010, **22**, 2206-2210.
11. H. Liu, Y. Ding, B. Yang, Z. Liu, Q. Liu and X. Zhang, *Sens. Actuators. B Chem.*, 2018, **271**, 336-345.
12. M. Chen, B. Yang, J. Zhu, H. Liu, X. Zhang, X. Zheng and Q. Liu, *Mater. Sci. Eng. C Mater. Biol. Appl.*, 2018, **90**, 610-620.
13. Q. Liu, Y. Yang, H. Li, R. Zhu, Q. Shao, S. Yang and J. Xu, *Biosens. Bioelectron.*, 2015, **64**, 147-153.
14. L. Zhang, L. Han, P. Hu, L. Wang and S. Dong, *Chem. Commun.*, 2013, **49**, 10480-10482.
15. J. Yang, L. Zheng, Y. Wang, W. Li, J. Zhang, J. Gu and Y. Fu, *Biosens. Bioelectron.*, 2016, **77**, 549-556.
16. X. X. Wang, Q. Wu, Z. Shan and Q. M. Huang, *Biosens. Bioelectron.*, 2011, **26**, 3614-3619.
17. D. Liao, J. Chen, H. Zhou, Y. Wang, Y. Li and C. Yu, *Anal. Chem.*, 2013, **85**, 2667-2672.
18. M. Rong, X. Song, T. Zhao, Q. Yao, Y. Wang and X. Chen, *J. Mater. Chem. C.*, 2015, **3**, 10916-10924.
19. C. Lei, Z. Wang, Z. Nie, H. Deng, H. Hu, Y. Huang and S. Yao, *Anal. Chem.*, 2015, **87**, 1974-1980.
20. H. Li, Y. Guo, L. Xiao and B. Chen, *Analyst*, 2014, **139**, 285-289.
21. Z. Chen, X. Ren, X. Meng, L. Tan, D. Chen and F. Tang, *Biosens. Bioelectron.*, 2013, **44**, 204-209.
22. W. Li, W. Li, Y. Hu, Y. Xia, Q. Shen, Z. Nie, Y. Huang and S. Yao, *Biosens. Bioelectron.*, 2013, **47**,

345-349.

23. X. Yan, Y. Song, X. Wu, C. Zhu, X. Su, D. Du and Y. Lin, *Nanoscale*, 2017, **9**, 2317-2323.
24. G. Liu, W. Guo and D. Song, *Biosens. Bioelectron.*, 2014, **52**, 360-366.
25. Q. Long, H. Li, Y. Zhang and S. Yao, *Biosens. Bioelectron.*, 2015, **68**, 168-174.
26. X. Yan, H. Li, X. Wang and X. Su, *Talanta*, 2015, **131**, 88-94.
27. Z.-L. Xu, H. Deng, X.-F. Deng, J.-Y. Yang, Y.-M. Jiang, D.-P. Zeng, F. Huang, Y.-D. Shen, H.-T. Lei, H. Wang and Y.-M. Sun, *Food Chem.*, 2012, **131**, 1569-1576.
28. S. Xu, C. Guo, Y. Li, Z. Yu, C. Wei and Y. Tang, *J. Hazard. Mater.*, 2014, **264**, 34-41.
29. H. Parham and N. Rahbar, *J. Hazard. Mater.*, 2010, **177**, 1077-1084.
30. X. Wang, Y. Yang, J. Dong, F. Bei and S. Ai, *Sens. Actuators. B Chem.*, 2014, **204**, 119-124.
31. J. Kumar, S. K. Jha and S. F. D'Souza, *Biosens. Bioelectron.*, 2006, **21**, 2100-2105.
32. X. Zhao, W. Kong, J. Wei and M. Yang, *Food. Chem.*, 2014, **162**, 270-276.
33. S. Nouanthavong, D. Nacapricha, C. S. Henry and Y. Sameenoi, *Analyst*, 2016, **141**, 1837-1846.
34. X. Liu, M. Song, T. Hou and F. Li, *ACS Sens.*, 2017, **2**, 562-568.
35. W. Lan, G. Chen, F. Cui, F. Tan, R. Liu and M. Yushupjiang, *Sensors*, 2012, **12**, 8477-8490.